



# Template synthesis and characterization of gold nano-wires and -particles in mesoporous channels of FSM-16

Hideobu Araki<sup>a</sup>, Atsushi Fukuoka<sup>a,\*</sup>, Yuzuru Sakamoto<sup>a</sup>, Shinji Inagaki<sup>b</sup>,  
Noriaki Sugimoto<sup>b</sup>, Yoshiaki Fukushima<sup>b</sup>, Masaru Ichikawa<sup>a,1</sup>

<sup>a</sup> Division of Chemistry, Graduate School of Science, and Catalysis Research Center, Hokkaido University, Sapporo 060-0811, Japan

<sup>b</sup> Toyota Central R&D Labs. Inc., Nagakute, Aichi 480-1192, Japan

Received 1 May 2002; received in revised form 4 November 2002; accepted 4 November 2002

Dedicated to late Professor Juro Horiuti in commemoration of his centennial birthday

## Abstract

Template synthesis of gold nano-wire and -particle onto mesoporous silica FSM-16 (Au/FSM-16) has been studied. Several Au/FSM-16 samples were prepared by chemical vapor deposition (CVD) or impregnation methods with subsequent reduction procedures. Organogold complex, dimethyl(hexafluoroacetylacetoato)gold(III) AuMe<sub>2</sub>(HFA), was adsorbed on FSM-16 by CVD, then irradiated by UV light, leading to the formation of Au nano-wires (diameter, 2.5 nm; mean length, 17.1 nm) in one-dimensional channels of FSM-16 (pore diameter, 2.7 nm). On the other hand, HAuCl<sub>4</sub> in aqueous solutions at various pH's was impregnated on FSM-16. The impregnated sample Au<sup>3+</sup>/FSM-16 prepared at pH 5 was reduced by H<sub>2</sub> at 673 K to give a mixture of Au nano-wires and -particles. In contrast, H<sub>2</sub>-reduction of Au<sup>3+</sup>/FSM-16 impregnated at pH 10 only gave homogeneously dispersed Au nano-particles in FSM-16 (mean diameter 1.7 nm). The size and morphology of the nanostructured Au metal is changed by pH of the aqueous HAuCl<sub>4</sub> solutions. The Au nano-wires and -particles were characterized by physicochemical methods such as TEM, XRD, EXAFS, and diffuse-reflectance UV-visible. CO oxidation was performed as a catalytic test reaction for the Au/FSM-16 composites.

© 2003 Elsevier Science B.V. All rights reserved.

**Keywords:** Mesoporous silica FSM-16; Gold catalyst; Nano-wire; Nano-particle; Template synthesis; CO oxidation

## 1. Introduction

Nanostructured metals and metal oxides have attracted current attention as key precursors to higher-ordered structures in a bottom-up approach of nanotechnology [1], and are expected to show unique magnetic, optical, electrical, mechanical, and catalytic

properties. However, precise control of the size and morphology of the nanostructured materials has been one of challenging topics since the pioneering work of Faraday on gold colloids in the 19th century [2]. The nano-wires and -particles have been prepared by a variety of methods such as thermal, photochemical, and electrochemical reductions of metal compounds. One of the most promising methods is template synthesis, in which the wires and particles are synthesized in uniform void spaces of porous materials [3]. Mesoporous silicas such as FSM-16 [4,5], MCM-41 [6], and SBA-15 [7] have been used as templates for

\* Corresponding authors.

E-mail addresses: [fukuoka@cat.hokudai.ac.jp](mailto:fukuoka@cat.hokudai.ac.jp) (A. Fukuoka), [michi@cat.hokudai.ac.jp](mailto:michi@cat.hokudai.ac.jp) (M. Ichikawa).

<sup>1</sup> Tel.: +81-11-706-3696; fax: +81-11-706-4957.

nanostructured metals. We have demonstrated that Pt nano-wires are synthesized by photoreduction of Pt ions impregnated on FSM-16 [8,9], and have shown the formation mechanism and the catalyses of the Pt nano-wires in the mesoporous silicas [10–13]. Nano-particles and short nano-wires of Au are also synthesized in mesoporous thin films [14]. Other groups also reported that the Pt nano-wires were formed by H<sub>2</sub>-reduction of Pt ions in the channels of MCM-41 [15,16].

Recently, Haruta have revealed that the catalytic performance of supported gold catalysts markedly depends on the degree of dispersion, support, and preparation methods [17]. The supported Au nano-particles show high catalytic activities in reactions such as CO oxidation and oxidation–decomposition of amines and organic halides. It was also reported that nanostructured Au metal with rod-like structure was formed on MCM-41, and their catalytic performance in CO oxidation was investigated [18]. Au nano-wires with a diameter of 7 nm were also prepared in the mesopores of SBA-15 [19].

In this work, we have studied preparation methods for selective synthesis of Au nano-wires and -particles in the mesopores of FSM-16. Organogold complex with high vapor pressure was used as a precursor for the chemical vapor deposition (CVD) method and tetrachloroauric acid as a precursor for the impregnation method. Characterization and catalytic performance of Au/FSM-16 nanocomposites were also explored.

## 2. Experimental

FSM-16 was prepared according to the published procedures [5]. The BET surface area was 950 m<sup>2</sup> g<sup>-1</sup> and the pore size was 2.7 nm. The powdered sample of FSM-16 was dried under vacuum (ca. 10<sup>-3</sup> Torr, 1 Torr = 133 Pa) at 623 K for 2 h. Dimethyl- (hexafluoroacetylacetoato)gold(III) AuMe<sub>2</sub>(HFA) (Fig. 1) of Tri Chemical Laboratory Inc. was used as received, and a Schlenk-type apparatus was used for the CVD experiments (Fig. 1) [20]. AuMe<sub>2</sub>(HFA) (1 Torr of vapor pressure at 308 K) was adsorbed on FSM-16 under reduced pressure at room temperature for 4 h, and excess Au complex was trapped by liquid N<sub>2</sub>. White AuMe<sub>2</sub>(HFA)/FSM-16 powder thus prepared in

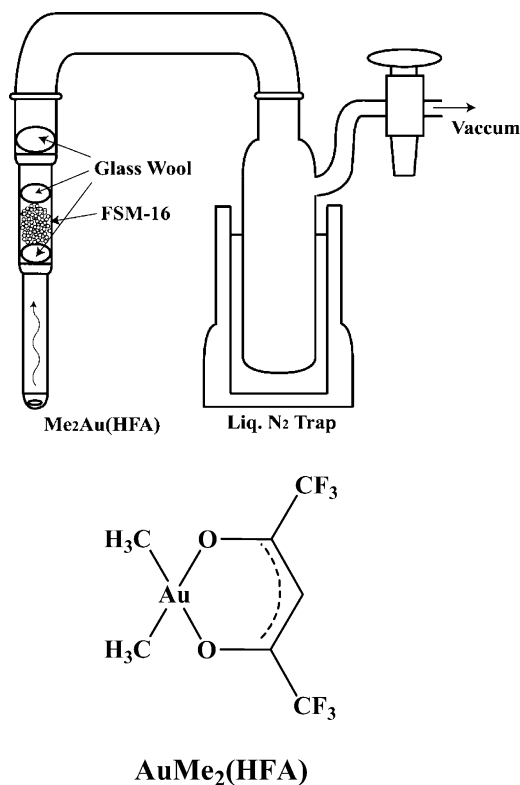


Fig. 1. Organogold complex AuMe<sub>2</sub>(HFA) and an apparatus for CVD.

a quartz cell was irradiated with a high pressure mercury lamp (Ushio UM-102, 100 W, 250–600 nm) under reduced pressure for 4 h. The white powder turned to pale purple by irradiation, showing the formation of Au metal. The powder was used for characterization after drying under vacuum.

Other Au/FSM-16 samples were prepared by the impregnation method as follows. The pH of aqueous HAuCl<sub>4</sub>·4H<sub>2</sub>O solution used in this work was originally 5. The solutions of pH 7 and 10 were prepared by adding NaOH to this HAuCl<sub>4</sub> solution. FSM-16 powder was added to the solution, and the mixture was stirred at room temperature for 24 h. The mixture was evaporated to dryness, and washed with water for removal of residual NaOH. Then the Au<sup>3+</sup>/FSM-16 (2.5 wt.% Au) samples were reduced by H<sub>2</sub>-reduction or photoreduction, where the H<sub>2</sub>-reduction was done in flowing H<sub>2</sub> (30 ml min<sup>-1</sup>) at 673 K for 2 h. In the photoreduction, Au<sup>3+</sup>/FSM-16 was exposed to water vapor (20 Torr) for 2 h and then methanol vapor

(100 Torr) for 2 h, and finally irradiated with the UV light for 24 h [11,13].

The reduced Au/FSM-16 samples were characterized by TEM, XRD, UV-visible, and EXAFS. TEM observation was performed by a Hitachi H-800 microscope at 200 kV. XRD patterns were obtained by a Rigaku Finiflex using Cu K $\alpha$  radiation ( $\lambda = 0.15418$  nm), and diffuse-reflectance UV-visible spectra by a Shimadzu UV-2200A. EXAFS spectra at Au L<sub>III</sub>-edge (11921 eV) were measured at the BL-10B station in the Photon Factory of High Energy Accelerator Research Organization (KEK-PF), Tsukuba, and the data were analyzed by a REX2000 program of Rigaku.

CO oxidation reaction was performed in a closed circulating reactor (volume 202 ml). Typically, 300 mg of Au/FSM-16 (2.5 wt.%) was used as a catalyst, and the reaction temperature was 343 K with initial pressures of  $p(\text{CO}) = 30$  Torr and  $p(\text{O}_2) = 150$  Torr. The concentrations of CO and O<sub>2</sub> were analyzed by a Hitachi 023 gas chromatograph with a thermal conductivity detector using a molecular sieve 13X column (4 m).

### 3. Results and discussion

#### 3.1. Synthesis and characterization of Au nano-wires and -particles in FSM-16

We have used various preparation methods to synthesize Au nano-wires and -particles in the mesopores of FSM-16. The preparation conditions and the mor-

phology and dimension of resulting Au metal are summarized in Table 1. In most cases Au particles were formed on the external surface of FSM-16; however, by tuning the deposition method of Au precursors and the reduction procedure, Au nano-wires and -particles can be prepared in the mesopores. The organogold complex AuMe<sub>2</sub>(HFA) has vapor pressure as high as 1 Torr at 308 K and high reactivity to photoirradiation to give Au metal, thus being suitable for the synthesis of nanostructured Au metal. According to this CVD-photoreduction strategy, irradiation of UV light to AuMe<sub>2</sub>(HFA) adsorbed on FSM-16 led to the formation of Au nano-wires in the mesopores of FSM-16 (Table 1, Entry 1). Fig. 2a is a TEM image of Au/FSM-16 (CVD), where Au nano-wires are observed as dark stripes. The mean diameter of the wires is 2.5 nm in accord with the pore diameter of FSM-16 (2.7 nm), indicating that the Au wires are embedded in the mesopores. The wire length is in the range of 10–50 nm with a mean length of 17 nm. In Fig. 2a, Au nano-particles in size of 5–10 nm are also observed possibly on the external surface of FSM-16, but the external particles are minor species. Therefore, the CVD with photo-induced decomposition is an effective method to prepare Au nano-wires in the void space of FSM-16.

In the impregnation method, HAuCl<sub>4</sub> undergoes ligand substitution with OH by increase of pH of the aqueous solutions, and Au(OH)<sub>3</sub> and [Au(OH)<sub>4</sub>]<sup>−</sup> thus formed may interact with surface OH groups of FSM-16 to give different dispersion and loading of the Au metal (Fig. 3) [18,21]. Fig. 2b shows a TEM image of the reduced sample Au/FSM-16 (pH 5) in

Table 1  
Synthesis of Au/FSM-16 nanocomposites under various preparation conditions

Entry	Precursor	Method	pH	Reduction method	Morphology of Au (dimension)	Sample name
1	AuMe <sub>2</sub> (HFA)	CVD	–	UV (4 h) <sup>a</sup>	Nano-wire (2.5 × 17.1 nm)	Au/FSM-16 (CVD)
2	HAuCl <sub>4</sub>	Impregnation	5	H <sub>2</sub> (673 K, 2 h)	Nano-wire (2.5 × 18.1 nm) <sup>b</sup>	Au/FSM-16 (pH 5)
3				O <sub>2</sub> (473 K, 2 h); H <sub>2</sub> (473 K, 2 h)	Nano-particle (16.0 nm)	Au/FSM-16 (pH 5-O)
4				UV (24 h) <sup>c</sup>	Nano-particle (19.2 nm)	
5	HAuCl <sub>4</sub>	Impregnation	7	H <sub>2</sub> (673 K, 2 h)	Nano-particle (2.3 nm)	Au/FSM-16 (pH 7)
6				UV (24 h) <sup>c</sup>	Nano-particle (18.5 nm)	
7	HAuCl <sub>4</sub>	Impregnation	10	H <sub>2</sub> (673 K)	Nano-particle (1.7 nm)	Au/FSM-16 (pH 10)
8				UV (24 h) <sup>c</sup>	Nano-particle (2.5 nm)	

<sup>a</sup> UV irradiation under reduced pressure.

<sup>b</sup> Nano-particles (ca. 10 nm) were also formed.

<sup>c</sup> UV irradiation in the presence of water (20 Torr) and methanol (100 Torr) vapors.

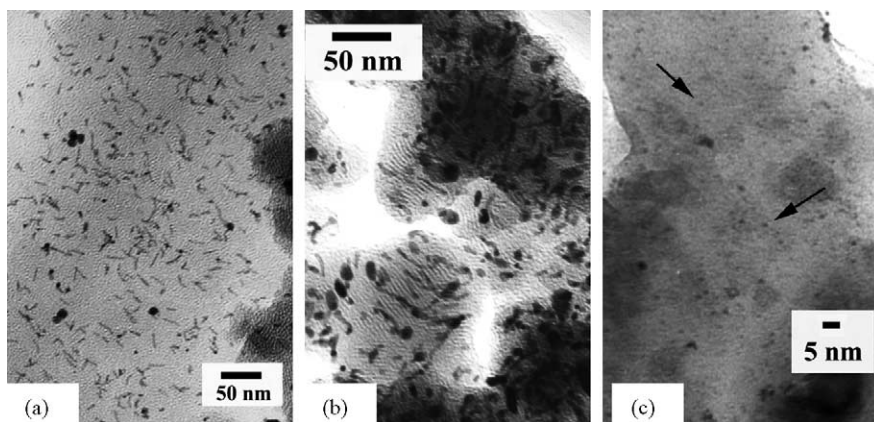


Fig. 2. TEM images of: (a) Au/FSM-16 (CVD); (b) Au/FSM-16 (pH 5); and (c) Au/FSM-16 (pH 10).

which both Au nano-wires and -particles were observed (Table 1, Entry 2). The Au nano-wires in this sample have a diameter of 2.5 nm and a mean length of 18.1 nm. However, the Au particles are as large as 10 nm, showing that they are located on the external surface of FSM-16. When the reduction methods were changed as shown in Entries 3 and 4 in Table 1, only nano-particles were formed on the external surface. When a solution of pH 7 was used for the impregnation method, the H<sub>2</sub>-reduced Au/FSM-16 (pH 7) gave Au nano-particles with a mean diameter of 2.3 nm in the mesopores (Table 1, Entry 5), while photoreduction yielded nano-particles (diameter 18.5 nm) on the external surface (Table 1, Entry 6).

From aqueous HAuCl<sub>4</sub> solution at pH 10 (Table 1, Entry 7), the H<sub>2</sub>-reduced Au/FSM-16 (pH 10) gave a TEM image of Fig. 2c. It is notable that small nano-particles of Au are homogeneously dispersed in the mesopores with a mean diameter of 1.7 nm. Photoreduction of Au<sup>3+</sup>/FSM-16 (pH 10) also gave Au

nano-particles with a mean diameter of 2.5 nm in the mesopores (Table 1, Entry 8).

The above results indicate that the preparation conditions of Au/FSM-16 give a great influence on the size and location of the Au metal. This difference may result from the migration of Au ions from the internal mesopores to the external surface during relatively slow photoreduction process. We propose that the Au hydroxides, Au(OH)<sub>3</sub> and [Au(OH)<sub>4</sub>]<sup>-</sup>, formed in neutral or basic solutions, can be highly dispersed in the mesopores of FSM-16, and the dispersed Au precursors are readily reduced by H<sub>2</sub> at 673 K to result in the formation of Au particles. The acidic solution at pH 5 gave ill-dispersed deposition of the Au ions in the impregnation, leading to the formation of a mixture of Au particles and wires both in the mesopores and on the external surface.

Fig. 4 shows XRD patterns of FSM-16, Au/FSM-16 (CVD), Au/FSM-16 (pH 5), and Au/FSM-16 (pH 10). In the low angle region, four peaks were observed at  $2\theta = 2.3, 4.1, 4.6,$  and  $6.1^\circ$  for FSM-16 as diffractions of (100), (110), (200), and (210) of a two-dimensional (2D) hexagonal structure. These peaks were also observed for the Au/FSM-16 samples, indicating that the pore structure of FSM-16 remained unchanged in the formation of the Au wires and particle. In the high region at  $2\theta = 30\text{--}90^\circ$ , typical peaks of fcc Au metal are observed, which are ascribed to (111), (200), (220), (311), and (222) diffractions.

Au L<sub>III</sub>-edge EXAFS was performed for the characterization of Au nano-wires and -particles. Fourier transforms of  $k^3$ -weighted EXAFS function  $\chi(k)$  of

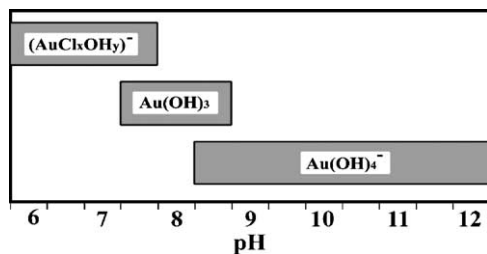


Fig. 3. Dependence of the ligand substitution of HAuCl<sub>4</sub> on the pH of its aqueous solutions [21].

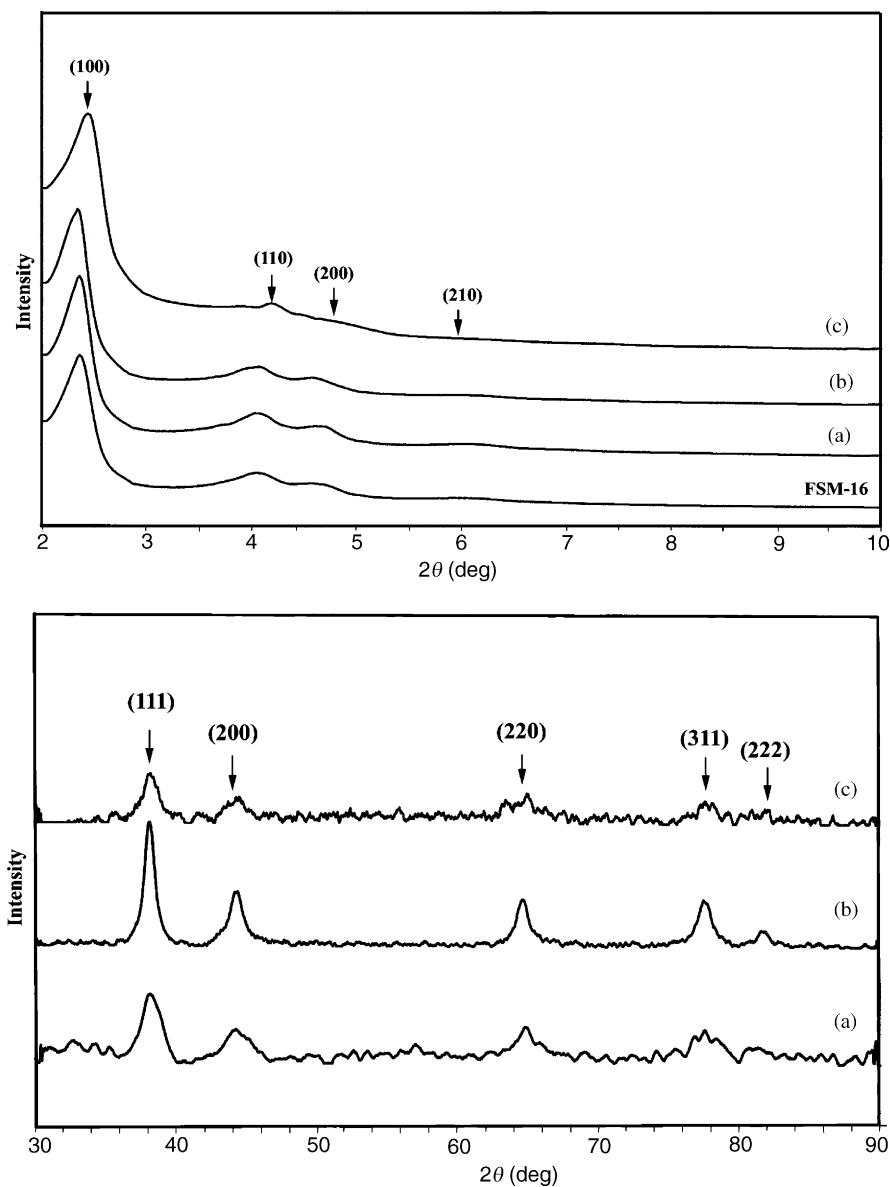


Fig. 4. XRD patterns of FSM-16: (a) Au/FSM-16 (CVD); (b) Au/FSM-16 (pH 5); and (c) Au/FSM-16 (pH 10).

Au foil, Au/FSM-16 (CVD), Au/FSM-16 (pH 5), and Au/FSM-16 (pH 10) are shown in Fig. 5, where large peaks are observed at 0.2–0.3 nm for the four samples. The peaks are assigned to the first shell of Au–Au in the curve-fitting analyses, but the contribution of Au–Cl or Au–O was negligible. Table 2 summarizes the results of curve-fitting analyses of the first shell of Au–Au. The Au–Au distances ( $R$ ) for the Au/FSM-16

samples are in the range of 0.284–0.288 nm, which are almost the same as that of Au foil (0.288 nm). Coordination numbers ( $N$ ) of the Au–Au are 9.5–10.8 for the Au/FSM-16 samples, being slightly lower than that of bulk Au ( $N = 12.0$ ). From EXAFS and XRD results, it is concluded that the Au precursors such as AuMe<sub>2</sub>(HFA), HAuCl<sub>4</sub>, and Au hydroxides are reduced to Au metal under our reduction conditions.

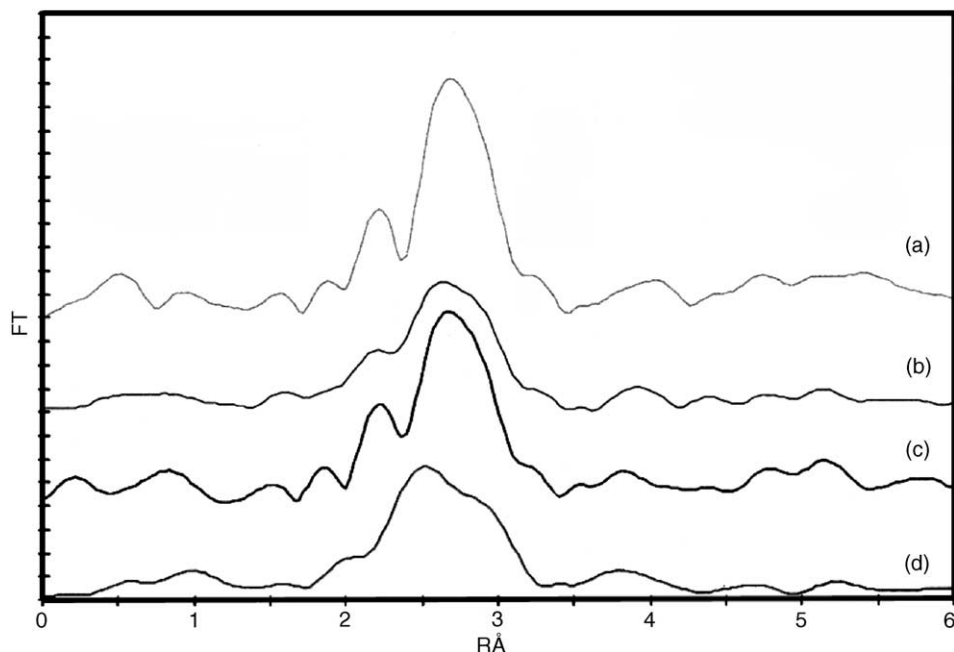


Fig. 5. Fourier transforms of  $k^3\chi(k)$  for: (a) Au foil; (b) Au/FSM-16 (CVD); (c) Au/FSM-16 (pH 5); and (d) Au/FSM-16 (pH 10).

Optical properties of the Au/FSM-16 samples were investigated by diffuse-reflectance UV-visible spectrometry (Fig. 6). For Au/FSM-16 (CVD) and Au/FSM-16 (pH 5) containing Au nano-wires, broad bands due to surface plasmon resonances were observed at 530–535 nm. Au nano-particles in size of 16 nm on the external surface of FSM-16, Au/FSM-16 (pH 5-O) (Table 1, Entry 3), gave a plasmon resonance at 512 nm. Therefore, it is noteworthy that Au/FSM-16 (CVD) and Au/FSM-16 (pH 5) containing Au nano-wires showed red-shift of the plasmon resonance by ca. 20 nm, while no band was observed at 400–800 nm for Au/FSM-16 (pH 10) because of a smaller diameter of the nano-particles (1.7 nm).

### 3.2. CO oxidation reaction by Au/FSM-16 catalysts

Supported Au nano-particles are known to be active catalysts for the CO oxidation reaction ( $\text{CO}_2 + 1/2\text{O}_2 \rightarrow \text{CO}_2$ ) [17,18], so that we tested the catalytic performance of Au/FSM-16 in this reaction. The reaction rate was obtained by the conversion of CO in the presence of excess  $\text{O}_2$ , and the first-order plots of the CO conversion yielded straight lines as shown in Fig. 7. Pseudo-first-order rate constants  $k_{\text{obs}}$  ( $\times 10^{-3} \text{ s}^{-1}$ ) from Fig. 7 were 0.012 for Au/FSM-16 (CVD), 0.025 for Au/FSM-16 (pH 5), 1.00 for Au/FSM-16 (pH 10), and 0.015 for Au/FSM-16 (pH 5-O), respectively. It is interesting to note that the rate constant of Au/FSM-16 (pH 10) is 40–80 times

Table 2  
Curve-fitting analyses for the first Au–Au shell for Au/FSM-16 nanocomposites

Sample	$N$	$R$ (nm)	$\sigma$ (nm)	$\Delta E_0$ (eV)	$R$ factor (%)
Au foil	$12.0 \pm 1.8$	$0.288 \pm 0.001$	0.006	0.3	0.4
Au/FSM-16 (CVD)	$9.5 \pm 2.2$	$0.286 \pm 0.001$	0.007	−0.4	1.6
Au/FSM-16 (pH 5)	$10.8 \pm 3.2$	$0.288 \pm 0.001$	0.007	1.0	2.2
Au/FSM-16 (pH 10)	$10.2 \pm 3.6$	$0.284 \pm 0.002$	0.007	−3.4	5.0

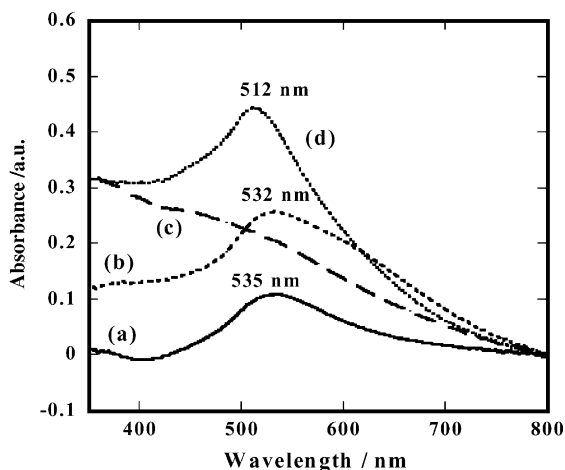


Fig. 6. Diffuse-reflectance UV-visible spectra of: (a) Au/FSM-16 (CVD); (b) Au/FSM-16 (pH 5); (c) Au/FSM-16 (pH 10); and (d) Au/FSM-16 (pH 5-O).

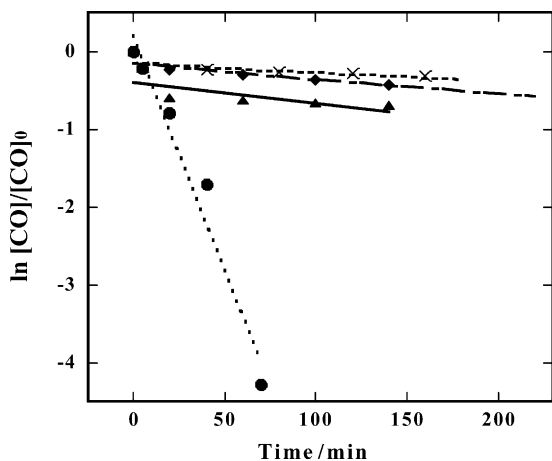


Fig. 7. First-order plots for CO oxidation by Au/FSM-16 catalysts. (x) Au/FSM-16 (CVD), (◆) Au/FSM-16 (pH 5), (●) Au/FSM-16 (pH 10), and (▲) Au/FSM-16 (pH 5-O).

higher than those of other three Au/FSM-16 catalysts. This result indicates that highly dispersed Au nano-particles as small as 2 nm in FSM-16 have a high catalytic activity in the CO oxidation reaction.

#### 4. Conclusions

It is demonstrated in this study that Au nano-wires are synthesized in the mesopores of FSM-16 by CVD

of AuMe<sub>2</sub>(HFA) complex and subsequent photoreduction, but Au nano-particles of 2 nm are obtained by impregnation of HAuCl<sub>4</sub> at pH 10 and H<sub>2</sub>-reduction. Thus, the selection of preparation conditions such as precursors, pH in case of impregnation of HAuCl<sub>4</sub>, and reduction methods has a significant effect on the size and morphology of the nanostructured Au metal. Mesoporous materials work as templates of the Au nano-wires and -particles. We are currently investigating the optical, electrical, magnetic, and catalytic applications of the nanocomposites.

#### Acknowledgements

This work was financially supported by a Grant-in-Aid for Scientific Research (C) from the Ministry of Education, Science, Sports and Culture, Japan (no. 13650836).

#### References

- [1] A.P. Alivisatos, *Science* 271 (1996) 933.
- [2] J.S. Bradley, in: G. Schmid (Ed.), *Clusters and Colloids*, VCH, Weinheim, 1994, p. 459 (Chapter 6).
- [3] M. Ichikawa, in: P. Braunstein, L.A. Oro, P.R. Raithby (Eds.), *Metal Clusters in Chemistry*, Wiley, Weinheim, 1999, p. 1273.
- [4] T. Yanagisawa, T. Shimizu, K. Kuroda, C. Kato, *Bull. Chem. Soc. Jpn.* 63 (1990) 988.
- [5] S. Inagaki, Y. Fukushima, K. Kuroda, *J. Chem. Soc., Chem. Commun.* (1993) 680.
- [6] C.T. Cresge, M.E. Leonowicz, W.J. Roth, J.C. Vartulli, J.S. Beck, *Nature* 359 (1992) 710.
- [7] D. Zhao, J. Feng, Q. Hua, N. Melosh, G.H. Fredrickson, B.F. Chmelka, G.D. Stucky, *Science* 279 (1998) 548.
- [8] M. Sasaki, M. Osada, N. Sugimoto, S. Inagaki, Y. Fukushima, A. Fukuoka, M. Ichikawa, *Microporous Mesoporous Mater.* 21 (1998) 597.
- [9] M. Sasaki, M. Osada, N. Higashimoto, T. Yamamoto, A. Fukuoka, M. Ichikawa, *J. Mol. Catal. A* 141 (1999) 223.
- [10] A. Fukuoka, N. Higashimoto, Y. Sakamoto, M. Sasaki, N. Sugimoto, S. Inagaki, Y. Fukushima, M. Ichikawa, *Catal. Today* 66 (2001) 23.
- [11] A. Fukuoka, N. Higashimoto, Y. Sakamoto, S. Inagaki, Y. Fukushima, M. Ichikawa, *Microporous Mesoporous Mater.* 48 (2001) 171.
- [12] A. Fukuoka, N. Higashimoto, Y. Sakamoto, S. Inagaki, Y. Fukushima, M. Ichikawa, *Topics Catal.* 18 (2002) 73.
- [13] A. Fukuoka, Y. Sakamoto, S. Guan, S. Inagaki, N. Sugimoto, Y. Fukushima, K. Hirahara, S. Iijima, M. Ichikawa, *J. Am. Chem. Soc.* 123 (2001) 3373.

- [14] A. Fukuoka, H. Araki, Y. Sakamoto, N. Sugimoto, H. Tsukada, Y. Kumai, Y. Akimoto, M. Ichikawa, *Nano Lett.* 2 (2002) 793.
- [15] C.H. Ko, R. Ryoo, *J. Chem. Soc., Chem. Commun.* (1996) 2467.
- [16] Z. Liu, Y. Sakamoto, T. Ohsuna, K. Hiraga, O. Terasaki, C.H. Ko, H.J. Shin, R. Ryoo, *Angew. Chem. Int. Ed.* 39 (2000) 3107.
- [17] M. Haruta, *Catal. Today* 36 (1997) 153.
- [18] M. Okumura, S. Tsubota, M. Iwamoto, M. Haruta, *Chem. Lett.* (1998) 315.
- [19] Y.-J. Han, J.M. Kim, G.D. Stucky, *Chem. Mater.* 12 (2000) 2068.
- [20] C.P. Mehnert, D.W. Weaver, J.Y. Ying, *J. Am. Chem. Soc.* 120 (1998) 12289.
- [21] R.J.H. Grisel, P.J. Kooyman, B.E. Nieuwenhuys, *J. Catal.* 191 (2000) 430.